

# Diffraction theory of an anisotropic circular cylinder

Michel Nevière, Evgeny Popov, and Philippe Boyer

*Institut Fresnel, Unité Mixte de Recherche Associée au Centre National de la Recherche Scientifique No. 6133, Université de Provence, Faculté des Sciences et Techniques de St. Jérôme, Avenue Escardille Normandie Niémen, 13397 Marseille Cedex 20, France*

Received July 15, 2005; revised January 5, 2006; accepted February 7, 2006; posted February 7, 2006 (Doc. ID 63503)

A fully analytical theory is developed to derive the field diffracted by an infinitely long circular cylinder made of an arbitrary anisotropic homogeneous material, illuminated by an arbitrary plane wave. © 2006 Optical Society of America

OCIS codes: 060.2310, 160.1190.

## 1. INTRODUCTION

The problem of diffraction of a plane wave by an infinitely long circular cylinder made of optically isotropic material was resolved more than a century ago in terms of Bessel functions.<sup>1</sup> However, only recently have studies of diffraction by cylinders composed of anisotropic materials appeared in the scientific literature. Reference 1 deals with a cylinder made of a uniaxial material with the optic and cylindrical axes coinciding and illuminated under incidence perpendicular to the axis. In this case, the cylinder diffracts light as if it were isotropic with two different permittivity values  $\epsilon_{\parallel}$  and  $\epsilon_{\perp}$ , depending on the polarization of the incident light, respectively, parallel or perpendicular to the cylindrical axis.

For more general anisotropy, the analysis becomes much more difficult. Several works deal with gyrotropic or uniaxial media where the optic axis does not coincide with the cylindrical axis.<sup>2,3</sup> In particular, Ref. 3 presents a detailed analysis in the case when the optic axis is perpendicular to the cylindrical axis. The approach presents an extension to conical (out-of-cross-section plane) incidence of the two-dimensional spectral approach, developed in Ref. 2. It will serve as a reference to validate the results presented in this paper.

As far as we know, there is no known solution of the problem of diffraction by a cylinder characterized by an arbitrary complex permittivity tensor  $\bar{\epsilon}$ . In a recent paper<sup>4</sup> we developed a theory of diffraction by a homogeneous arbitrary anisotropic sphere, based on the general expression of the field inside a general anisotropic material,<sup>5</sup> developed in terms of plane waves. Here we apply a similar approach in cylindrical coordinates, which are well adapted to applying the boundary conditions on the cylinder surface. However, the invariance of the object along its axis makes a big difference when compared with a sphere.

## 2. PRESENTATION OF THE PROBLEM

We consider an infinitely long circular cylinder with axis  $Oz$  and radius  $R$ . Figure 1 represents its truncated part.

The exterior is a homogeneous isotropic medium with absolute permittivity  $\epsilon_{\text{ext}}$ . An incident plane wave with unit amplitude and with wave vector  $\mathbf{k}_{\text{inc}}$  propagates in the direction  $\hat{\mathbf{r}}_{\text{inc}} = \mathbf{k}_{\text{inc}}/|\mathbf{k}_{\text{inc}}|$ , defined by the angles  $\theta_{\text{inc}} \in [0, \pi]$  and  $\varphi_{\text{inc}} \in [0, 2\pi]$ . Its polarization vector  $\hat{\mathbf{e}}_{\text{inc}}$  can be arbitrary oriented in the plane transverse to  $\mathbf{k}_{\text{inc}}$ . The interior of the cylinder is filled with an arbitrary (lossy or lossless) anisotropic homogeneous material, characterized by the relative permittivity tensor,

$$\bar{\epsilon} = \begin{bmatrix} \epsilon_{xx} & \epsilon_{xy} & \epsilon_{xz} \\ \epsilon_{yx} & \epsilon_{yy} & \epsilon_{yz} \\ \epsilon_{zx} & \epsilon_{zy} & \epsilon_{zz} \end{bmatrix}, \quad (1)$$

in which no symmetry relation is assumed *a priori*. We only notice that the homogeneity of the material implies the independence of the components of  $\bar{\epsilon}$  with respect to the Cartesian coordinates.

By introducing the transformation matrix  $\mathfrak{R}$ , which links Cartesian to cylindrical coordinates, the expression of the permittivity tensor in cylindrical coordinates is given by the relation

$$\tilde{\epsilon} = \mathfrak{R} \bar{\epsilon} \mathfrak{R}^T, \quad (2)$$

where T stands for transpose. If the circumflex denotes the unit vectors, the transformation matrix components are given by the scalar products between the basis vectors  $\{\hat{\mathbf{x}}, \hat{\mathbf{y}}, \hat{\mathbf{z}}\}$  and  $\{\hat{\rho}, \hat{\varphi}, \hat{\mathbf{z}}\}$ :

$$\mathfrak{R} = \begin{bmatrix} \hat{\rho} \cdot \hat{\mathbf{x}} & \hat{\rho} \cdot \hat{\mathbf{y}} & \hat{\rho} \cdot \hat{\mathbf{z}} \\ \hat{\varphi} \cdot \hat{\mathbf{x}} & \hat{\varphi} \cdot \hat{\mathbf{y}} & \hat{\varphi} \cdot \hat{\mathbf{z}} \\ \hat{\mathbf{z}} \cdot \hat{\mathbf{x}} & \hat{\mathbf{z}} \cdot \hat{\mathbf{y}} & \hat{\mathbf{z}} \cdot \hat{\mathbf{z}} \end{bmatrix} = \begin{bmatrix} \cos \varphi & \sin \varphi & 0 \\ -\sin \varphi & \cos \varphi & 0 \\ 0 & 0 & 1 \end{bmatrix}. \quad (3)$$

Since the cylindrical coordinate system is orthogonal, it is not necessary to distinguish between covariant and contravariant tensorial components and thus they will be denoted by subscripts. It is worth noting that while  $\epsilon_{ij}$  are independent of  $x, y, z$ , they depend on  $\varphi$  through Eq. (3).

Because of the invariance of the diffraction problem with respect to the  $z$  coordinate, the  $z$  dependence of the

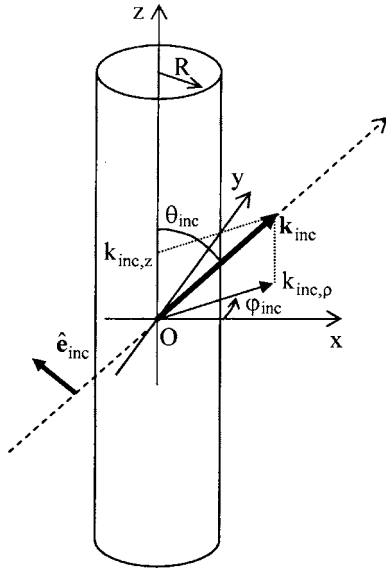


Fig. 1. Circular cylinder illuminated under oblique incidence.

scattered field is determined by the  $z$  dependence of the incident field,<sup>6</sup> given by  $\exp(ik_{\text{inc},z}z)$  with

$$k_{\text{inc},z} = k_{\text{inc}} \cos \theta_{\text{inc}}. \quad (4)$$

### 3. EXPRESSION OF THE FIELD INSIDE A HOMOGENEOUS ANISOTROPIC MEDIUM

Let us at first find the form of a single plane wave propagating inside a homogeneous anisotropic material, expressed in cylindrical coordinates, and presenting a  $z$  dependence given by Eq. (4).

#### A. Propagation Equation

In an anisotropic medium, the Maxwell equations lead to the following propagation equation:

$$\text{curl curl } \mathbf{E} - k_0^2 \tilde{\epsilon} \mathbf{E} = 0, \quad (5)$$

where  $k_0$  is the vacuum wavenumber. Because of the homogeneity of the medium, in each point defined by its radius vector  $\mathbf{r}$  we look for solutions in the form of a plane wave with a wave vector  $\mathbf{k}$ :

$$\mathbf{E}(\mathbf{k}, \mathbf{r}) = \mathbf{A} \exp(i\mathbf{k} \cdot \mathbf{r}). \quad (6)$$

The solution of the diffraction problem will be found as a superposition of such plane waves.

Recalling that  $\text{curl}[\mathbf{A} \exp(i\mathbf{k} \cdot \mathbf{r})] = i\mathbf{k} \times \mathbf{A} \exp(i\mathbf{k} \cdot \mathbf{r})$ , Eq. (5) leads to

$$\mathbf{k} \times (\mathbf{k} \times \mathbf{A}) + k_0^2 \tilde{\epsilon} \mathbf{A} = 0. \quad (7)$$

By using a tensorial product of two vectors, we construct a tensor  $(\mathbf{k}\mathbf{k})$  whose  $(i,j)$  component is equal to  $k_i k_j$ , and then Eq. (7) can be written in the form

$$[k^2 \mathbf{I} - (\mathbf{k}\mathbf{k}) - k_0^2 \tilde{\epsilon}] \mathbf{A} = 0, \quad (8)$$

where  $k = |\mathbf{k}| = [\text{Tr}(\mathbf{k}\mathbf{k})]^{1/2}$  and  $\mathbf{I}$  is the unit matrix.

To have a nontrivial solution of Eq. (8), it is necessary to fulfill the following condition:

$$\det[k^2 \mathbf{I} - (\mathbf{k}\mathbf{k}) - k_0^2 \tilde{\epsilon}] = 0. \quad (9)$$

This equation determines the wavenumbers  $k$  of the plane waves propagating in a given direction in a homogeneous anisotropic medium. Then Eq. (8) gives the proper vectors of polarization for each plane wave. It is interesting to point out that  $k$  represents a nonlinear eigenvalue of the tensor  $[(\mathbf{k}\mathbf{k}) + k_0^2 \tilde{\epsilon}]$ .<sup>7</sup>

#### B. Finding the Wavenumbers

Equations (8) and (9) are valid in any coordinate system. The determination of the wavenumbers  $k$  is especially easy in spherical coordinates, since there the tensor  $(\mathbf{k}\mathbf{k})$  has a single nonnull component.<sup>5</sup> In principle, it should be possible to use these values, obtained for each direction of propagation  $(\varphi, \theta)$ ; however, this would give different values of  $k_z$ . We need to fix this as long as the  $z$  dependence of the field is equal to the  $z$  dependence of the incident field [Eq. (4)]. We are thus obliged to solve Eqs. (8) and (9) in cylindrical coordinates. To this aim, we fix the angle of propagation  $\varphi$  in the  $Oxy$  plane and we state that the vertical component  $k_z$  of the unknown wave vector  $\mathbf{k}$  is equal to  $k_{\text{inc},z}$ . The components of  $\mathbf{k}$  can be expressed using the unknown angle of propagation  $\theta$  with respect to the  $z$  axis. Denoting its tangent as  $t$  ( $t = \tan \theta$ ), we obtain

$$\mathbf{k}_\rho = k_z t g \theta = k_z t, \quad k_\varphi = 0, \quad k = k_z / \cos \theta = k_z \sqrt{1 + t^2},$$

$$\forall \theta \neq \pi/2,$$

$$k_\rho = k, \quad k_z = 0, \quad \theta = \pi/2. \quad (10)$$

Thus the tensor  $(\mathbf{k}\mathbf{k})$  takes the form

$$(\mathbf{k}\mathbf{k}) = \begin{bmatrix} k_\rho^2 & 0 & k_z k_\rho \\ 0 & 0 & 0 \\ k_z k_\rho & 0 & k_z^2 \end{bmatrix} = \begin{bmatrix} k_z^2 t^2 & 0 & k_z^2 t \\ 0 & 0 & 0 \\ k_z^2 t & 0 & k_z^2 \end{bmatrix}, \quad (11)$$

and Eq. (9) is written as

$$\det \left[ k_z^2 (1 + t^2) \mathbf{I} - \begin{bmatrix} k_z^2 t^2 & 0 & k_z^2 t \\ 0 & 0 & 0 \\ k_z^2 t & 0 & k_z^2 \end{bmatrix} - k_0^2 \tilde{\epsilon} \right] = 0. \quad (12)$$

This is a fourth-order algebraic equation for  $t$ . Its four solutions  $t_j$ ,  $j=1, \dots, 4$ , represent four possible directions of propagation for each fixed value of  $k_z$  and  $\varphi$ . However, as long as  $k_z$  participates in Eq. (12) only through its square  $k_z^2$ , two of the roots, say  $t_1$  and  $t_2$ , correspond to positive values of  $k_z$  and two roots ( $t_3$  and  $t_4$ ) correspond to negative  $k_z$ . Once  $t_1$  and  $t_2$  are determined, two values  $k_1$  and  $k_2$  of  $k$  are deduced from Eqs. (10).

The case when the incident wave propagates in the  $Oxy$  plane needs a special treatment. With  $k_z=0$  (and thus  $k_\rho = k$ ), Eq. (9) is simplified to

$$\det \left[ \begin{bmatrix} 0 & 0 & 0 \\ 0 & k^2 & 0 \\ 0 & 0 & k^2 \end{bmatrix} - k_0^2 \tilde{\epsilon} \right] = 0, \quad (13)$$

which is a biquadratic equation with respect to  $k$ . This equation has four solutions  $k_j$ ,  $j=1, \dots, 4$ , having, in

couples, opposite signs. The opposite signs correspond to waves propagating in opposite directions, so that it is necessary to preserve only a single representative (say,  $k_1$  and  $k_2$ ) of each couple, say the one with positive real parts.

### C. Finding the Polarization Vectors

Once the wavenumbers  $k_1$  and  $k_2$  are chosen, Eq. (8) could be used to obtain the polarization vectors  $\mathbf{A}_1$  and  $\mathbf{A}_2$ . This could easily be done when we notice that  $\mathbf{A}_1$  is the eigenvector of the matrix  $k_1^2 \mathbf{1} - (\mathbf{k}_1 \mathbf{k}_1) - k_0^2 \tilde{\epsilon}$ , corresponding to the zero eigenvalue of this matrix, which exists due to Eq. (9). The same applies for  $\mathbf{A}_2$  when  $k = k_2$  is chosen. In the case when  $k_1 \neq k_2$ , each matrix  $k_j^2 \mathbf{1} - (\mathbf{k}_j \mathbf{k}_j) - k_0^2 \tilde{\epsilon}$ ,  $j=1,2$ , has a single zero eigenvalue (see Appendix A), so that the choice of the corresponding vector  $\mathbf{A}_j$  is unique. If  $k_1 = k_2$ , the matrices  $k_j^2 \mathbf{1} - (\mathbf{k}_j \mathbf{k}_j) - k_0^2 \tilde{\epsilon}$  for  $j=1$  and  $j=2$  are identical, they have a double zero eigenvalue, and there are two vectors, which could be chosen linearly independent (i.e., mutually orthogonal). This points out that in the degenerated case (corresponding to an isotropic medium or a uniaxial medium when the ordinary and the extraordinary waves propagate along the optic axis) the two independent polarizations of the electric field vector are mutually orthogonal (and orthogonal to  $\mathbf{k}$ ) and can be arbitrarily chosen in the plane perpendicular to  $\mathbf{k}$ . In the general case, the two vectors  $\mathbf{A}_1$  and  $\mathbf{A}_2$  are uniquely determined (each within a multiplicative constant) and could be nonorthogonal. Appendix B provides a direct analytical method to determine the components of the eigenvectors.

As long as each eigenvector is determined within a constant, we introduce normalized polarization vectors  $\Gamma_j$ ,  $j=1,2$ , and electric field amplitudes  $\tilde{A}_j$  such that

$$\mathbf{A}_j(k_z, \varphi) = \tilde{A}_j(k_z, \varphi) \Gamma_j(k_z, \varphi). \quad (14)$$

### D. General Form of the Field inside the Anisotropic Material

The electric field at an arbitrary point  $M$  in space having radius vector  $\mathbf{r}_{OM}$  can be expressed as a superposition of plane waves propagating in all possible directions. Each direction of propagation is characterized by a couple of wavenumbers  $k_1$  and  $k_2$ , directions of polarization  $\Gamma_1$  and  $\Gamma_2$ , and amplitudes  $\tilde{A}_1$  and  $\tilde{A}_2$ . However, when  $k_z = k_{inc,z}$  is fixed, the possible directions are characterized by the angle of propagation  $\varphi$  in the  $Oxy$  plane. Figure 2 presents a schematic view of the point  $M$  with its coordinates and the scattered field wave vector  $\mathbf{k}$ , represented in local coordinates  $(x', y', z')$ . In what follows we skip the  $k_z$  dependence of the wave characteristics. The superposition with respect to  $\varphi$  contains two values of  $k$  for each  $\varphi$ :

$$\mathbf{E}(\mathbf{r}_{OM}) = \sum_{j=1}^2 \int_0^{2\pi} d\varphi \tilde{A}_j(\varphi) \Gamma_j(\varphi) \exp[i\mathbf{k}_j(\varphi) \cdot \mathbf{r}_{OM}], \quad (15)$$

where  $\mathbf{k}_j(\varphi) = \mathbf{k}_{j,\rho}(\varphi) \hat{\rho} + k_z \hat{z}$ . During numerical treatment, the integration along  $\varphi$  is replaced by a discrete sum over  $\nu$  from 1 to  $N_\varphi$  with  $\varphi$  taking  $N_\varphi$  discrete values:

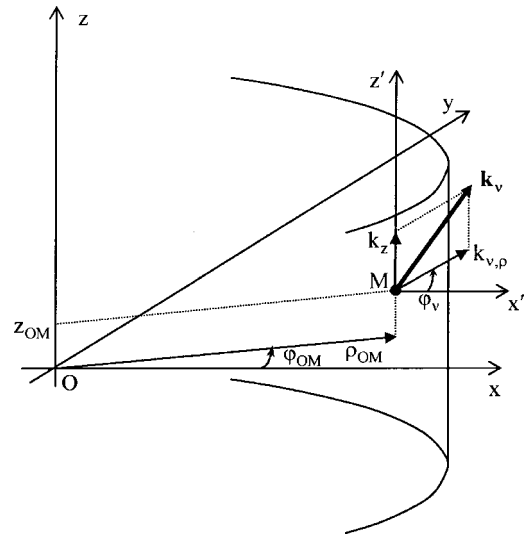


Fig. 2. Zoom of Fig. 1 with the coordinates of point  $M$  and the wave-vector components.

$$\varphi_\nu = 2\pi(\nu - 1)/N_\varphi. \quad (16)$$

As a result, it is necessary to make the following substitutions:

$$\begin{aligned} \tilde{A}_{j,\nu} &= \tilde{A}_j(\varphi_\nu) d\varphi = \tilde{A}_j(\varphi_\nu) \frac{2\pi}{N_\varphi}, & \Gamma_{j,\nu} &= \Gamma_j(\varphi_\nu), \\ \mathbf{k}_{j,\nu} &= \mathbf{k}_j(\varphi_\nu). \end{aligned}$$

## 4. FOURIER-BESSEL EXPANSION OF THE FIELD

### A. Field inside the Isotropic Medium

Outside the cylinder the field consists of an incident plane wave and scattered (diffracted) field. We assume an incident field with a unit amplitude and polarization vector  $\hat{\mathbf{e}}_{inc}$ ; the electric field of the incident wave has the form

$$\begin{aligned} \mathbf{E}^{inc}(\mathbf{r}_{OM}) &= \hat{\mathbf{e}}_{inc} \exp(i\mathbf{k}_{inc} \cdot \mathbf{r}_{OM}) \\ &= \hat{\mathbf{e}}_{inc} \exp(ik_{inc,\rho} \hat{\rho}_{inc} \cdot \rho_{OM}) \exp(ik_z z_{OM}). \end{aligned} \quad (17)$$

Note that  $k_z = k_{inc,z}$  and  $\mathbf{k}_{inc} = k_{inc,\rho}(\varphi) \hat{\rho} + k_z \hat{z}$ .

The  $2\pi$  periodicity with respect to  $\varphi_{OM}$  allows us to represent the vectorial components of the total field by a Fourier series:

$$E_j(\mathbf{r}_{OM}) = \sum_{n=-\infty}^{+\infty} E_{j,n}(\rho_{OM}) \exp(in\varphi_{OM}) \exp(ik_z z_{OM}). \quad (18)$$

Recalling the Fourier-Bessel expansion,

$$\exp(i\zeta \cos \psi) = \sum_{n=-\infty}^{+\infty} i^n J_n(\zeta) \exp(in\psi), \quad (19)$$

where  $J_n$  are the Bessel functions, the field expansion of the incident wave can be written in the form

$$\mathbf{E}^{\text{inc}}(\mathbf{r}_{\text{OM}}) = \hat{\mathbf{e}}_{\text{inc}} \sum_{n=-\infty}^{+\infty} i^n J_n(k_{\text{inc},\rho} \rho_{\text{OM}}) \times \exp[in(\varphi_{\text{OM}} - \varphi_{\text{inc}})] \exp(ik_z z_{\text{OM}}), \quad (20)$$

where  $\varphi_{\text{inc}}$  is the angle between the  $x$  axis and the projection of  $\mathbf{k}_{\text{inc}}$  onto the  $Oxy$  plane. Let us consider the  $z$  components of the electric and magnetic fields. As long as  $e_{\text{inc},z}$  is independent of the position of  $M$ , Eq. (20) gives

$$E_{z,n}^{\text{inc}}(\mathbf{r}_{\text{OM}}) = A_{e,n}^{\text{inc}} J_n(k_{\text{inc},\rho} \rho_{\text{OM}}),$$

$$A_{e,n}^{\text{inc}} = \hat{\mathbf{e}}_{\text{inc}} \cdot \hat{\mathbf{z}} i^n \exp(-in\varphi_{\text{inc}}). \quad (21)$$

A similar expression is obtained for the magnetic field<sup>8</sup>:

$$i\omega\mu_0 H_{z,n}^{\text{inc}}(\mathbf{r}_{\text{OM}}) = A_{h,n}^{\text{inc}} J_n(k_{\text{inc},\rho} \rho_{\text{OM}}),$$

$$A_{h,n}^{\text{inc}} = ik_{\text{inc}}(\hat{\mathbf{r}}_{\text{inc}} \times \hat{\mathbf{e}}_{\text{inc}}) \cdot \hat{\mathbf{z}} i^n \exp(-in\varphi_{\text{inc}}). \quad (22)$$

The scattered field has a quite similar form, obtained from Eqs. (21) and (22) by substituting the Bessel functions with Hankel functions  $H_n^+$ , which represent a field propagating toward  $\rho \rightarrow \infty$ , and replacing the known incident amplitudes with unknown amplitudes  $B_{e,n}$  and  $B_{h,n}$ , so that the Fourier components of the total field become

$$E_{z,n}^{\text{ext}}(\mathbf{r}_{\text{OM}}) = A_{e,n}^{\text{inc}} J_n(k_{\text{inc},\rho} \rho_{\text{OM}}) + B_{e,n} H_n^+(k_{\text{inc},\rho} \rho_{\text{OM}}), \quad (23)$$

$$i\omega\mu_0 H_{z,n}^{\text{ext}}(\mathbf{r}_{\text{OM}}) = A_{h,n}^{\text{inc}} J_n(k_{\text{inc},\rho} \rho_{\text{OM}}) + B_{h,n} H_n^+(k_{\text{inc},\rho} \rho_{\text{OM}}), \quad (24)$$

where the  $z$  dependence given by the factor  $\exp(ik_z z_{\text{OM}})$  is omitted.

The Maxwell equations written in cylindrical coordinates allow us to derive  $E_\varphi$  and  $H_\varphi$ :

$$E_\varphi = \frac{1}{k_{\text{inc},\rho}^2} \left( \frac{ik_z}{\rho} \frac{\partial E_z}{\partial \varphi} - i\omega\mu_0 \frac{\partial H_z}{\partial \rho} \right), \quad (25)$$

$$H_\varphi = \frac{1}{k_{\text{inc},\rho}^2} \left( \frac{ik_z}{\rho} \frac{\partial H_z}{\partial \varphi} + i\omega\epsilon_{\text{ext}} \frac{\partial E_z}{\partial \rho} \right), \quad (26)$$

which leads to

$$E_{\varphi,n} = \frac{-1}{k_{\text{inc},\rho}^2} \left\{ \left[ nk_z A_{e,n}^{\text{inc}} \frac{J_n(k_{\text{inc},\rho} \rho_{\text{OM}})}{\rho_{\text{OM}}} + k_{\text{inc},\rho} A_{h,n}^{\text{inc}} J_n'(k_{\text{inc},\rho} \rho_{\text{OM}}) \right] + \left[ nk_z B_{e,n} \frac{H_n^+(k_{\text{inc},\rho} \rho_{\text{OM}})}{\rho_{\text{OM}}} + k_{\text{inc},\rho} B_{h,n} H_n^{+'}(k_{\text{inc},\rho} \rho_{\text{OM}}) \right] \right\}, \quad (27)$$

$$i\omega\mu_0 H_{\varphi,n} = \frac{-1}{k_{\text{inc},\rho}^2} \left\{ \left[ nk_z A_{h,n}^{\text{inc}} \frac{J_n(k_{\text{inc},\rho} \rho_{\text{OM}})}{\rho_{\text{OM}}} + k_{\text{inc},\rho}^2 A_{e,n}^{\text{inc}} J_n'(k_{\text{inc},\rho} \rho_{\text{OM}}) \right] + \left[ nk_z B_{h,n} \frac{H_n^+(k_{\text{inc},\rho} \rho_{\text{OM}})}{\rho_{\text{OM}}} + k_{\text{inc},\rho}^2 B_{e,n} H_n^{+'}(k_{\text{inc},\rho} \rho_{\text{OM}}) \right] \right\}. \quad (28)$$

These formulas will be used in Section 5 to apply the boundary conditions on the cylinder surface, keeping in mind the  $z$ -dependence term  $\exp(ik_z z_{\text{OM}})$ .

## B. Field Inside the Cylinder

Making use of Eq. (19), the field in Eq. (15), after discretization of the integral, takes the form

$$\mathbf{E}(\mathbf{r}_{\text{OM}}) = \sum_{j=1}^2 \sum_{\nu=1}^{N_\varphi} \tilde{A}_{j,\nu} \Gamma_{j,\nu} \sum_{n=-\infty}^{+\infty} i^n J_n(k_{j,\nu,\rho} \rho_{\text{OM}}) \exp[in(\varphi_{\text{OM}} - \varphi_\nu)], \quad (29)$$

where the  $z$  dependence is omitted. Thus the cylindrical components of  $\mathbf{E}$  depend on the polarization vectors  $\Gamma_{j,\nu}$ . While each  $\Gamma_{j,\nu}$  is expressed in the coordinate set  $(\hat{\rho}_\nu, \hat{\varphi}_\nu, \hat{\mathbf{z}})$ , it is necessary to obtain its projections onto the local set  $(\hat{\rho}_{\text{OM}}, \hat{\varphi}_{\text{OM}}, \hat{\mathbf{z}})$ , linked with the point  $M$ . We obtain

$$\begin{aligned} \Gamma_{j,\nu} \cdot \hat{\rho}_{\text{OM}} &= (\Gamma_{j,\nu,\rho} \hat{\rho}_\nu + \Gamma_{j,\nu,\varphi} \hat{\varphi}_\nu) \cdot \hat{\rho}_{\text{OM}} \\ &= \Gamma_{j,\nu,\rho} \cos(\varphi_{\text{OM}} - \varphi_\nu) + \Gamma_{j,\nu,\varphi} \sin(\varphi_{\text{OM}} - \varphi_\nu), \end{aligned} \quad (30)$$

$$\begin{aligned} \Gamma_{j,\nu} \cdot \hat{\varphi}_{\text{OM}} &= (\Gamma_{j,\nu,\rho} \hat{\rho}_\nu + \Gamma_{j,\nu,\varphi} \hat{\varphi}_\nu) \cdot \hat{\varphi}_{\text{OM}} \\ &= -\Gamma_{j,\nu,\rho} \sin(\varphi_{\text{OM}} - \varphi_\nu) + \Gamma_{j,\nu,\varphi} \cos(\varphi_{\text{OM}} - \varphi_\nu), \end{aligned} \quad (31)$$

$$\Gamma_{j,z} \cdot \hat{\mathbf{z}} = \Gamma_{j,\nu,z}. \quad (32)$$

Projecting Eq. (29) onto  $\hat{\rho}_{\text{OM}}$ , using Eq. (30), and introducing the coefficients,

$$\alpha_{o,n,j,\nu} = \Gamma_{j,\nu,\rho} i^n \exp(-in\varphi_\nu), \quad (33)$$

$$\alpha_{h,n,j,\nu} = ik_{j,\nu,\rho} \Gamma_{j,\nu,\varphi} i^n \exp(-in\varphi_\nu), \quad (34)$$

$$\alpha_{e,n,j,\nu} = \Gamma_{j,\nu,z} i^n \exp(-in\varphi_\nu), \quad (35)$$

the first component of  $\mathbf{E}$  takes the form

$$\begin{aligned}
E_\rho(\mathbf{r}_{\text{OM}}) = & \sum_{j=1}^2 \sum_{\nu=1}^{N_\varphi} \frac{\tilde{A}_{j,\nu}}{2} \left\{ \sum_{n=-\infty}^{+\infty} -i \left( \alpha_{o,n+1,j,\nu} - \frac{\alpha_{h,n+1,j,\nu}}{k_{j,\nu,\rho}} \right) \right. \\
& \times J_n(k_{j,\nu,\rho} \rho_{\text{OM}}) \exp[i(n+1)\varphi_{\text{OM}}] \\
& + \sum_{n=-\infty}^{+\infty} i \left( \alpha_{o,n-1,j,\nu} + \frac{\alpha_{h,n-1,j,\nu}}{k_{j,\nu,\rho}} \right) J_n(k_{j,\nu,\rho} \rho_{\text{OM}}) \\
& \left. \times \exp[i(n-1)\varphi_{\text{OM}}] \right\}. \quad (36)
\end{aligned}$$

Changing  $n$  into  $n-1$  in the first sum and into  $n+1$  in the second sum and using the relations between Bessel functions  $J_{n-1}(\xi) + J_{n+1}(\xi) = 2nJ_n(\xi)/\xi$  and  $J_{n-1}(\xi) - J_{n+1}(\xi) = 2J'_n(\xi)$ , one obtains for the  $n$ th Fourier components of  $E_\rho$

$$\begin{aligned}
E_{\rho,n}(\mathbf{r}_{\text{OM}}) = & -i \sum_{j=1}^2 \sum_{\nu=1}^{N_\varphi} \tilde{A}_{j,\nu} \left[ \frac{nJ_n(k_{j,\nu,\rho} \rho_{\text{OM}})}{k_{j,\nu,\rho}^2 \rho_{\text{OM}}} \right. \\
& \left. - \alpha_{o,n,j,\nu} J'_n(k_{j,\nu,\rho} \rho_{\text{OM}}) \right]. \quad (37)
\end{aligned}$$

In a similar way, by putting Eq. (31) into Eq. (29), the  $n$ th Fourier component of  $E_\varphi$  can be obtained:

$$\begin{aligned}
E_{\varphi,n}(\mathbf{r}_{\text{OM}}) = & \sum_{j=1}^2 \sum_{\nu=1}^{N_\varphi} \tilde{A}_{j,\nu} \left[ \alpha_{o,n,j,\nu} \frac{nJ_n(k_{j,\nu,\rho} \rho_{\text{OM}})}{k_{j,\nu,\rho} \rho_{\text{OM}}} \right. \\
& \left. - \frac{\alpha_{h,n,j,\nu}}{k_{j,\nu,\rho}} J'_n(k_{j,\nu,\rho} \rho_{\text{OM}}) \right], \quad (38)
\end{aligned}$$

while finding  $E_{z,n}$  is straightforward:

$$E_{z,n}(\mathbf{r}_{\text{OM}}) = \sum_{j=1}^2 \sum_{\nu=1}^{N_\varphi} \tilde{A}_{j,\nu} \alpha_{e,n,j,\nu} J_n(k_{j,\nu,\rho} \rho_{\text{OM}}). \quad (39)$$

We recall that the  $z$  dependence given by the factor  $\exp(ik_z z_{\text{OM}})$  is omitted in Eqs. (29)–(39). However, this dependence is required to calculate the components of  $\mathbf{H}$  using the Maxwell equations, which provide the following links:

$$H_\varphi = \frac{1}{i\omega\mu_0} \left( \frac{\partial E_\rho}{\partial z} - \frac{\partial E_z}{\partial \rho} \right), \quad (40)$$

$$H_z = \frac{1}{i\omega\mu_0} \left( \frac{E_\varphi}{\rho} + \frac{\partial E_\varphi}{\partial \rho} - \frac{1}{\rho} \frac{\partial E_\rho}{\partial \varphi} \right). \quad (41)$$

Substituting Eqs. (37) and (38) into Eq. (41) and taking into account the Bessel equation  $J''_n(\xi) + J'_n(\xi)/\xi - (n^2/\xi^2 - 1)J_n(\xi) = 0$  and the fact that  $(J'_n/\xi)' - J'_n/\xi + J_n/\xi^2 = 0$ , we obtain

$$i\omega\mu_0 H_{z,n}(\mathbf{r}_{\text{OM}}) = \sum_{j=1}^2 \sum_{\nu=1}^{N_\varphi} \tilde{A}_{j,\nu} \alpha_{h,n,j,\nu} J_n(k_{j,\nu,\rho} \rho_{\text{OM}}). \quad (42)$$

A similar procedure applied to Eq. (40) by using Eqs. (37) and (39) gives

$$\begin{aligned}
i\omega\mu_0 H_{\varphi,n}(\mathbf{r}_{\text{OM}}) = & - \sum_{j=1}^2 \sum_{\nu=1}^{N_\varphi} \tilde{A}_{j,\nu} \left\{ k_z \left[ n \alpha_{h,n,j,\nu} \frac{J_n(k_{j,\nu,\rho} \rho_{\text{OM}})}{k_{j,\nu,\rho}^2 \rho_{\text{OM}}} \right. \right. \\
& \left. \left. - \alpha_{o,n,j,\nu} J'_n(k_{j,\nu,\rho} \rho_{\text{OM}}) \right] \right. \\
& \left. + k_{j,\nu,\rho} \alpha_{e,n,j,\nu} J'_n(k_{j,\nu,\rho} \rho_{\text{OM}}) \right\}. \quad (43)
\end{aligned}$$

## 5. BOUNDARY CONDITIONS

The continuity of the components of  $\mathbf{E}$  and  $\mathbf{H}$  tangential to the cylinder surface results in the continuity of each of their Fourier components:

$$\begin{aligned}
A_{e,n}^{\text{inc}} J_n(k_{\text{inc},\rho} R) + B_{e,n} H_n^+(k_{\text{inc},\rho} R) \\
= \sum_{j=1}^2 \sum_{\nu=1}^{N_\varphi} \tilde{A}_{j,\nu} \alpha_{e,n,j,\nu} J_n(k_{j,\nu,\rho} R), \quad (44)
\end{aligned}$$

$$\begin{aligned}
nk_z A_{e,n}^{\text{inc}} \frac{J_n(k_{\text{inc},\rho} R)}{k_{\text{inc},\rho}^2 R} + A_{h,n}^{\text{inc}} \frac{J'_n(k_{\text{inc},\rho} R)}{k_{\text{inc},\rho}} \\
+ nk_z B_{e,n} \frac{H_n^+(k_{\text{inc},\rho} R)}{k_{\text{inc},\rho}^2 R} + B_{h,n} \frac{H_n^{+'}(k_{\text{inc},\rho} R)}{k_{\text{inc},\rho}} \\
= \sum_{j=1}^2 \sum_{\nu=1}^{N_\varphi} \tilde{A}_{j,\nu} \left[ -n \alpha_{o,n,j,\nu} \frac{J_n(k_{j,\nu,\rho} R)}{k_{j,\nu,\rho} R} + \alpha_{h,n,j,\nu} \frac{J'_n(k_{j,\nu,\rho} R)}{k_{j,\nu,\rho}} \right], \quad (45)
\end{aligned}$$

$$\begin{aligned}
A_{h,n}^{\text{inc}} J_n(k_{\text{inc},\rho} R) + B_{h,n} H_n^+(k_{\text{inc},\rho} R) \\
= \sum_{j=1}^2 \sum_{\nu=1}^{N_\varphi} \tilde{A}_{j,\nu} \alpha_{h,n,j,\nu} J_n(k_{j,\nu,\rho} R), \quad (46)
\end{aligned}$$

$$\begin{aligned}
nk_z A_{h,n}^{\text{inc}} \frac{J_n(k_{\text{inc},\rho} R)}{k_{\text{inc},\rho}^2 R} + k_{\text{inc},\rho}^2 A_{e,n}^{\text{inc}} \frac{J'_n(k_{\text{inc},\rho} R)}{k_{\text{inc},\rho}} \\
+ nk_z B_{h,n} \frac{H_n^+(k_{\text{inc},\rho} R)}{k_{\text{inc},\rho}^2 R} + k_{\text{inc},\rho}^2 B_{e,n} \frac{H_n^{+'}(k_{\text{inc},\rho} R)}{k_{\text{inc},\rho}} \\
= \sum_{j=1}^2 \sum_{\nu=1}^{N_\varphi} \tilde{A}_{j,\nu} \left[ nk_z \alpha_{h,n,j,\nu} \frac{J_n(k_{j,\nu,\rho} R)}{k_{j,\nu,\rho}^2 R} \right. \\
\left. + (k_{j,\nu,\rho} \alpha_{e,n,j,\nu} - k_z \alpha_{o,n,j,\nu}) J'_n(k_{j,\nu,\rho} R) \right]. \quad (47)
\end{aligned}$$

Equations (44)–(47) are valid for each  $n$ . Numerical treatment requires truncation in  $n$ , say from  $-N$  to  $+N$ . This will limit the number of equations to  $4(2N+1)$ , and the number of unknown scattered amplitudes in the external medium  $B_{e,n}$  and  $B_{h,n}$  will become equal to  $2(2N+1)$ . In addition, the number of unknowns inside the cylinder  $\tilde{A}_{j,\nu}$  is equal to  $2N_\varphi$ . To obtain a Cramer set, it is necessary to chose a discretization in  $\varphi$  depending on  $N$  such that  $N_\varphi = 2N+1$ , i.e., that the number of the unknown field components inside and outside are equal. With this condition applied, all the field amplitudes can be found by solving a

linear algebraic set, i.e., by a single matrix inversion. It is worth noticing that the Fourier components of the field outside the cylinder are coupled through the field inside the cylinder, as long as  $\tilde{A}_{j,\nu}$  are identical for each  $n$ . If the cylinder consists of optically uniaxial material with the optic axis parallel to the geometrical axis, this coupling disappears, as discussed in Section 6.

### 6. UNIAXIAL MATERIAL

When the cylinder consists of a material having uniaxial anisotropy with the optic axis parallel to the cylinder axis, the permittivity tensor takes a simple diagonal form:

$$\bar{\epsilon} = \begin{bmatrix} \epsilon_x & 0 & 0 \\ 0 & \epsilon_x & 0 \\ 0 & 0 & \epsilon_z \end{bmatrix}, \tag{48}$$

and each direction of propagation is characterized by two wavenumbers<sup>9</sup>:

$$k_1 = k_0 \sqrt{\epsilon_x},$$

$$\frac{1}{k_2^2(\theta)} = \frac{1}{k_0^2} \left( \frac{\sin^2 \theta}{\epsilon_z} + \frac{\cos^2 \theta}{\epsilon_x} \right) \tag{49}$$

corresponding to the so-called ordinary and extraordinary wave, respectively. They form two surfaces in the  $k$  space, a sphere (with radius equal to  $k_0 \sqrt{\epsilon_x}$ ) for the ordinary wave and an ellipsoid of revolution (around the  $k_z$  axis) for the extraordinary wave, which ellipsoid has an axis equal to  $k_0 \sqrt{\epsilon_z}$  along  $k_\rho$  and  $k_0 \sqrt{\epsilon_x}$  along  $k_z$  (Fig. 3). The wavenumber  $k_1$  of the ordinary wave does not depend on the direction of propagation, and its polarization vector is perpendicular to the direction of propagation and to the optical axis<sup>4,9</sup>:

$$tg \theta_1 \equiv t_1 = \sqrt{(k_0^2 \epsilon_x - k_z^2)/k_z},$$

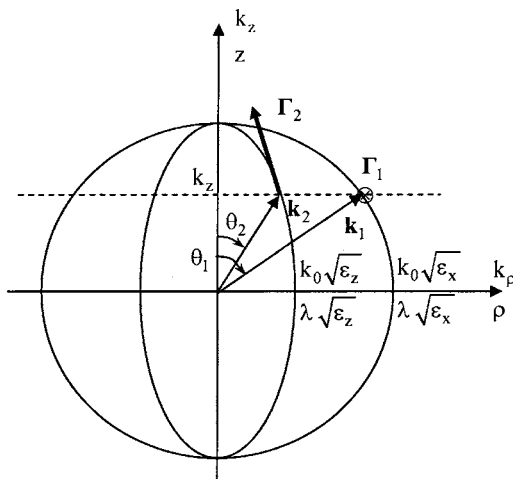


Fig. 3. Index surfaces in the  $k$  space (upper notation in each pair) and in the coordinate space (lower notation) and the wave vectors and the polarization vectors in the coordinate space.

$$\Gamma_{1,\nu} = \hat{\phi}_\nu. \tag{50}$$

The wavenumber and polarization vector of the extraordinary wave depend on the polar angle  $\theta$ , but are independent of  $\varphi$ . For each value of  $k_z$ , there are two possible directions of propagation, as can be observed in Fig. 3, except for the cases when  $k_z=0$  and  $k_z=k_0 \sqrt{\epsilon_x}$ . It can be shown that, using Eq. (34) of Ref. 4,

$$tg \theta_2 \equiv t_2 = \frac{\sqrt{\epsilon_z(k_0^2 \epsilon_x - k_z^2)/\epsilon_x}}{k_z},$$

$$\Gamma_2 = \frac{-t_2 \frac{k_z^2}{k_0^2 \epsilon_x - k_z^2} \hat{\rho} + \hat{z}}{\sqrt{1 + \left( t_2 \frac{k_z^2}{k_0^2 \epsilon_x - k_z^2} \right)^2}}$$

$$= \frac{-\epsilon_z \hat{\rho} + \epsilon_x t_2 \hat{z}}{\sqrt{(\epsilon_x t_2)^2 + \epsilon_z^2}}. \tag{51}$$

As can be observed,  $\Gamma_{2,\nu} \perp \hat{\phi}_\nu$ , which can be expected by taking into account Eqs. (50). If, instead of  $k_1/k_0$  and  $k_2/k_0$  in Eqs. (49), we take the ratio  $r/\lambda$  of the distance from the origin and the wavelength, these equations represent two surfaces in the direct space of the coordinates, a sphere and an ellipsoid of revolution, identical to the surfaces in the  $k$  space. These surfaces in the direct space are called index surfaces and it can be shown that the polarization vectors are tangential to them, as represented schematically in Fig. 3.

Taking all this into consideration, it is possible to significantly simplify the form of the wave expansion inside the uniaxial material and thus to simplify the boundary conditions. We observe, at first, that Eqs. (33)–(35) become

$$a_{o,n,1,\nu} = a_{e,n,1,\nu} = a_{h,n,2,\nu} = 0, \tag{52}$$

$$a_{h,n,1,\nu} = ik_{1,\rho} i^n \exp(-in\varphi_\nu), \tag{53}$$

$$a_{e,n,2,\nu} = \Gamma_{2,z} i^n \exp(-in\varphi_\nu),$$

$$a_{o,n,2,\nu} = \Gamma_{2,\rho} i^n \exp(-in\varphi_\nu). \tag{54}$$

As long as the arguments of Bessel functions participating in the field expansion inside the cylinder, Eqs. (37)–(39), (42), and (43), do not depend on  $\varphi_\nu$ , it is possible to extract them from the sum over  $\nu$  and to introduce new amplitudes, which are proportional to the  $n$ th Fourier components of the field amplitudes  $\tilde{A}_{j,\nu}$  with respect to  $\varphi_{OM}$ :

$$A_{h,n}^{(1)} = \sum_\nu \tilde{A}_{1,\nu} a_{h,n,1,\nu} = ik_{1,\rho} i^n \sum_\nu \tilde{A}_{1,\nu} \exp(-in\varphi_\nu), \tag{55}$$

$$A_{e,n}^{(1)} = \sum_\nu \tilde{A}_{2,\nu} a_{e,n,2,\nu} = i^n \Gamma_{2,z} \sum_\nu \tilde{A}_{2,\nu} \exp(-in\varphi_\nu), \tag{56}$$

$$A_{o,n}^{(1)} = \sum_{\nu} \tilde{A}_{2,\nu} \alpha_{o,n,2,\nu} = i^n \Gamma_{2,\rho} \sum_{\nu} \tilde{A}_{2,\nu} \exp(-in\varphi_{\nu}). \quad (57)$$

In addition, using Eqs. (51), one obtains the following links:

$$A_{o,n}^{(1)} = \frac{\Gamma_{2,\rho}}{\Gamma_{2,z}} A_{e,n}^{(1)} = -\frac{\epsilon_z k_z}{\epsilon_x k_{\rho}} A_{e,n}^{(1)}. \quad (58)$$

In isotropic materials this means that the polarization of the electric field is transverse to the direction of propagation. Using these new amplitudes, the boundary conditions are simplified to give

$$A_{e,n}^{\text{inc}} J_n(k_{\text{inc},\rho} R) + B_{e,n} H_n^+(k_{\text{inc},\rho} R) = A_{e,n}^{(1)} J_n(k_{2,\rho} R), \quad (59)$$

$$\begin{aligned} nk_z A_{e,n}^{\text{inc}} \frac{J_n(k_{\text{inc},\rho} R)}{k_{\text{inc},\rho}^2 R} + A_{h,n}^{\text{inc}} \frac{J'_n(k_{\text{inc},\rho} R)}{k_{\text{inc},\rho}} \\ + nk_z B_{e,n} \frac{H_n^+(k_{\text{inc},\rho} R)}{k_{\text{inc},\rho}^2 R} + B_{h,n} \frac{H_n^+(k_{\text{inc},\rho} R)}{k_{\text{inc},\rho}} \\ = nk_z \frac{\epsilon_z}{\epsilon_x} A_{e,n}^{(1)} \frac{J_n(k_{2,\rho} R)}{k_{2,\rho}^2 R} + A_{h,n}^{(1)} \frac{J'_n(k_{1,\rho} R)}{k_{1,\rho}}, \end{aligned} \quad (60)$$

$$A_{h,n}^{\text{inc}} J_n(k_{\text{inc},\rho} R) + B_{h,n} H_n^+(k_{\text{inc},\rho} R) = A_{h,n}^{(1)} J_n(k_{1,\rho} R), \quad (61)$$

$$\begin{aligned} nk_z A_{h,n}^{\text{inc}} \frac{J_n(k_{\text{inc},\rho} R)}{k_{\text{inc},\rho}^2 R} + k_{\text{inc}}^2 A_{e,n}^{\text{inc}} \frac{J_n(k_{\text{inc},\rho} R)}{k_{\text{inc},\rho}} \\ + nk_z B_{h,n} \frac{H_n^+(k_{\text{inc},\rho} R)}{k_{\text{inc},\rho}^2 R} + k_{\text{inc}}^2 B_{e,n} \frac{H_n^+(k_{\text{inc},\rho} R)}{k_{\text{inc},\rho}} \\ = nk_z A_{h,n}^{(1)} \frac{J_n(k_{1,\rho} R)}{k_{1,\rho} R} + \left( k_{2,\rho}^2 + \frac{\epsilon_z}{\epsilon_x} k_{2,z}^2 \right) A_{e,n}^{(1)} \frac{J'_n(k_{2,\rho} R)}{k_{2,\rho}}. \end{aligned} \quad (62)$$

These equations are uncoupled with respect to  $n$ , so that for each value of  $n$  it is necessary to solve only a system of four equations. They have a form quite similar to the isotropic case, which can be obtained by taking into account that  $\epsilon_x = \epsilon_z$  and thus  $k_2 = k_1$ . However, in both uniaxial or isotropic cases, if the incidence lies outside of the cross-section plane (i.e.,  $k_z \neq 0$ ), the fundamental cases of polarization (indices  $e$  and  $h$ ) remain coupled.

If, in addition, the incident wave vector is perpendicular to the  $z$  axis, the fundamental polarizations are decoupled and diffract independently in both uniaxial or isotropic cases. This fact can be observed by imposing  $k_z = 0$  in Eqs. (59)–(62) and using  $k_{\text{inc},\rho} = k_{\text{inc}}$ ,  $k_{1,\rho} = k_1$ , and  $k_{2,\rho} = k_2$ :

$$A_{e,n}^{\text{inc}} J_n(k_{\text{inc}} R) + B_{e,n} H_n^+(k_{\text{inc}} R) = A_{e,n}^{(1)} J_n(k_2 R), \quad (63)$$

$$\frac{1}{k_{\text{inc}}} [A_{h,n}^{\text{inc}} J'_n(k_{\text{inc}} R) + B_{h,n} H_n^+(k_{\text{inc}} R)] = \frac{1}{k_1} A_{h,n}^{(1)} J'_n(k_1 R), \quad (64)$$

$$A_{h,n}^{\text{inc}} J_n(k_{\text{inc}} R) + B_{h,n} H_n^+(k_{\text{inc}} R) = A_{h,n}^{(1)} J_n(k_1 R), \quad (65)$$

$$k_{\text{inc}} [A_{e,n}^{\text{inc}} J'_n(k_{\text{inc}} R) + B_{e,n} H_n^+(k_{\text{inc}} R)] = k_2 A_{e,n}^{(1)} J'_n(k_2 R). \quad (66)$$

In that case the set reduces to the well-known equation published in Ref. 1. It appears that Eqs. (63) and (66) are uncoupled from Eqs. (64) and (65). It is necessary to point out that this decoupling of the fundamental polarizations when considering incidence in the cross-section plane does not occur in the case of general anisotropy. Even if Eqs. (44)–(47) are rather simplified when  $k_z = 0$ , the fact that the polarization vectors depend on  $\varphi$  will couple the  $h$  and the  $e$  amplitudes outside the cylinder through the amplitudes  $\tilde{A}_{j,\nu}$  inside it.

## 7. NUMERICAL APPLICATIONS

As a first validation test of the theory, we have chosen one of the rare cases found in the literature that represents numerical examples available for comparison. This is the case treated by Monzon<sup>3</sup> and it concerns conical diffraction of a plane wave (wavelength  $\lambda = 2$ ) on an uniaxially anisotropic circular cylinder, having a radius  $R = 1$  and optical axis along  $Ox$ , perpendicular to the symmetry axis  $Oz$ . The nonnull components of the relative permittivity tensor are  $\epsilon_{xx} = 4.87526$  and  $\epsilon_{yy} = \epsilon_{zz} = 5.29$ , and the external medium is vacuum. The direction of the incident wave vector (Fig. 1) is defined by  $\varphi_{\text{inc}} = 90^\circ$  and  $\theta_{\text{inc}} = 30^\circ$ . The incident polarization is perpendicular to the  $z$  axis,  $\hat{\mathbf{e}}_{\text{inc}} \perp \hat{\mathbf{z}}$ , and the amplitude of the magnetic field vector is normalized to unity  $|\mathbf{H}^{\text{inc}}| = 1$ . We compare our results with the ones of Fig. 6 of Ref. 3. The differential cross section (DCS) is given by

$$\sigma_H(\varphi) = \frac{\sqrt{2/\pi}}{\omega \mu_0 \sin(\theta_{\text{inc}})} \left| \sum_{n=-N}^{+N} (-i)^n B_{h,n} e^{in\varphi} \right|, \quad (67)$$

$$\sigma_E(\varphi) = \sqrt{\frac{\epsilon_0}{\mu_0} \frac{\sqrt{2/\pi}}{\sin(\theta_{\text{inc}})}} \left| \sum_{n=-N}^{+N} (-i)^n B_{e,n} e^{in\theta} \right|. \quad (68)$$

Figure 4 shows  $\sigma_H$  and  $\sigma_E$ , calculated with  $N = 20$  and compared with the DCSs of a cylindrical cylinder filled with an isotropic medium having  $\epsilon = 5.29$ . The results for the anisotropic cylinder are exactly the same as obtained in Ref. 3.

A parameter important in numerical applications is the convergence rate with respect to the truncation value of  $N$ . Figure 5 represents  $\sigma_H$  as a function of  $N$  and shows that is sufficient to take  $N = 9$  to obtain correct results. The convergence rate is a little slower than for the isotropic case, but this could be explained by the gap in the components of the relative permittivity tensor  $\epsilon_{xx}$  and  $\epsilon_{yy} (= \epsilon_{zz})$ . In fact, the convergence is determined by both the optical contrast between the external medium and the cylinder and by the difference between the components of the permittivity tensor. This is illustrated in Figs. 6 and 7. When keeping the same value of  $\epsilon_{xx}$  and increasing four times the other two components,  $\epsilon_{yy} = \epsilon_{zz} = 21.16$ , the convergence rate reduces and it is necessary to use  $N$  as high as 22 to obtain relevant results (Fig. 6). When reducing the difference between  $\epsilon_{xx} (= 20.74526)$  and  $\epsilon_{yy} (= \epsilon_{zz} = 21.16)$ , the convergence rate improves (Fig. 7) and approaches the convergence rate of the case given in Fig. 5,

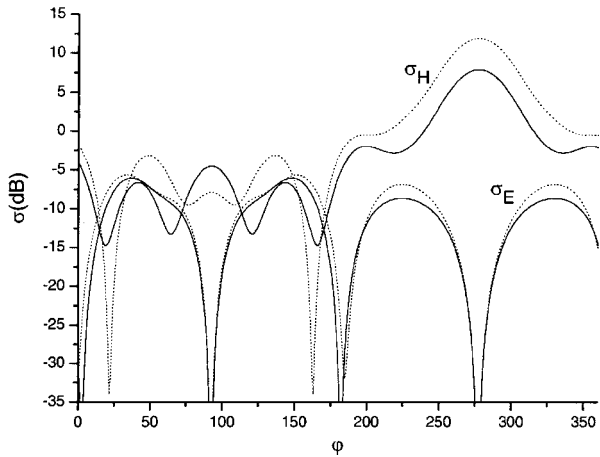


Fig. 4. DCS of the magnetic ( $\sigma_H$ ) and the electric ( $\sigma_E$ ) fields for a circular cylinder with  $R=1$  having  $Oz$  as symmetry axis and filled with an uniaxial anisotropic medium with  $\epsilon_{xx}=4.87526$  and  $\epsilon_{yy}=\epsilon_{zz}=5.29$ , and  $\epsilon_{ext}=1$ , compared with DCSs of an isotropic circular cylinder with  $\epsilon=5.29$  ( $R=1$ ). The incident plane-wave parameters are  $\lambda=2$ ,  $\varphi_{inc}=90^\circ$ , and  $\theta_{inc}=30^\circ$ , and the polarization is perpendicular to the  $z$  axis. Solid curves, anisotropic case; dotted curves, isotropic case.

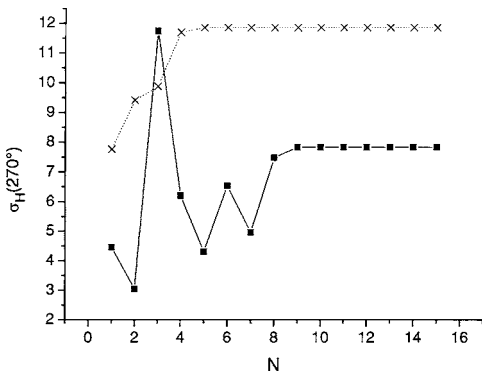


Fig. 5. Convergence test of  $\sigma_H$  as a function of the order  $N$  of the truncated Fourier series for the point  $\varphi=270^\circ$  in Fig. 4. Solid curve, anisotropic case; dotted curve, isotropic case.

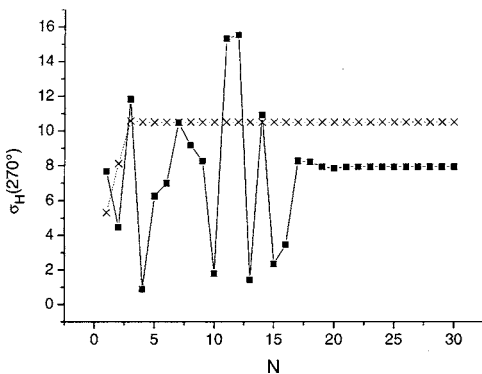


Fig. 6. Same as in Fig. 5, but with different anisotropy,  $\epsilon_{xx}=4.87526$  and  $\epsilon_{yy}=\epsilon_{zz}=21.16$  (solid curve). The dotted curve represents the isotropic case illustrated in Fig. 5. The other parameters are the same as in Fig. 4.

even when keeping a very high optical contrast between the external and the internal media.

In the last example, we demonstrate the possibility of the method to analyze a biaxial anisotropy, when all three diagonal components of the permittivity tensor are differ-

ent. Figure 8 represents the DCSs (calculated with  $N=20$ ) for a biaxial anisotropic case with  $\epsilon_{xx}=2$ ,  $\epsilon_{yy}=2.25$ , and  $\epsilon_{zz}=2.5$ , compared with an isotropic medium ( $\epsilon=2.25$ ). The corresponding convergence test for  $\sigma_H(270^\circ)$  is shown in Fig. 9. When compared with Fig. 5, one observes that the convergence rate is almost the same as for a uniaxial cylinder.

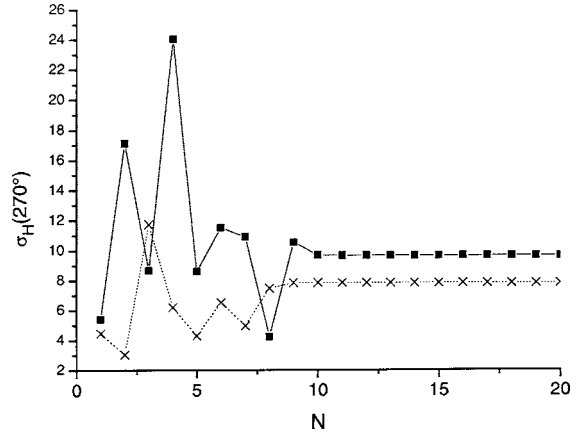


Fig. 7. Same as in Fig. 6, but with  $\epsilon_{xx}=20.74526$  and  $\epsilon_{yy}=\epsilon_{zz}=21.16$  (solid curve). The dotted curve represents the anisotropic case illustrated in Fig. 5.

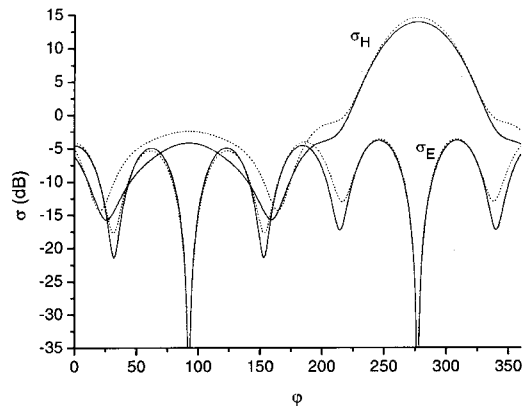


Fig. 8. DCS of the magnetic ( $\sigma_H$ ) and the electric ( $\sigma_E$ ) fields for a circular cylinder with  $R=1$  and filled with an anisotropic medium with  $\epsilon_{xx}=2$ ,  $\epsilon_{yy}=2.25$ , and  $\epsilon_{zz}=2.5$  and compared with a DCS of an isotropic circular cylinder with  $\epsilon=2.25$ . The other parameters are the same as in Fig. 4.

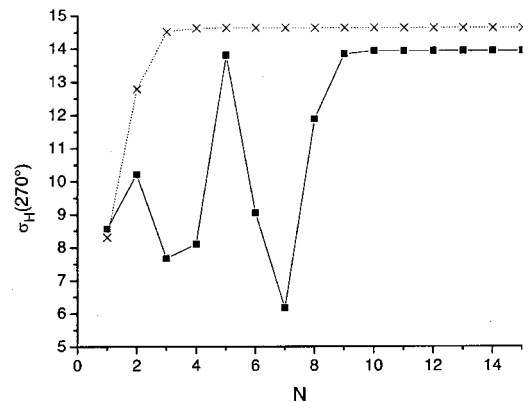


Fig. 9. Convergence test with respect to the order  $N$  of the truncated Fourier series of  $\sigma_H$  in the point  $\varphi=270^\circ$  in Fig. 8. Solid curve, anisotropic case; dotted curve, isotropic case.



## 8. CONCLUSION

Using a plane-wave expansion in an arbitrary homogeneous anisotropic material, we are able to derive equations determining the diffraction by a circular optically anisotropic cylinder. Finding the diffracted amplitudes reduces to a matrix inversion, the size of which is determined by the required number of Fourier components of the field. The theory is somewhat similar to the theory of diffraction by an optically anisotropic sphere. However, it appears more difficult to determine the wavenumbers and polarization vectors in cylindrical geometry, when compared with spherical coordinates. But, since the cylindrical geometry preserves the wavenumber  $k_z$  along its axis, it requires discretization of space directions inside the anisotropic material to be done along the azimuthal angle only, while the spherical geometry needs discretization along both the azimuthal and the polar angle.

Numerical studies confirm the validity of the method with respect to already published results and show relatively rapid convergence rates, which require inversion of a matrix of a size typically of the order of  $100 \times 100$ .

The theory presented in this paper can be directly applied to the study of guided-wave propagation and thus the modal structure of optically anisotropic fibers. It can be further generalized to model light diffraction by arbitrary (noncircular) cross-section optically anisotropic cylinders.

## APPENDIX A: DEGENERACY OF WAVENUMBERS

After having determined the two wavenumbers  $k_1$  and  $k_2$  by solving a fourth-order algebraic Eq. (9), then Eq. (8) can be used to numerically obtain the polarization vectors  $\mathbf{A}_1$  and  $\mathbf{A}_2$ , each of which represents the eigenvector corresponding to the zero eigenvalue, say,  $\gamma_1$ , of Eq. (8). The aim of this appendix is to prove that if  $k_1 \neq k_2$  then  $\gamma_1 = 0$  is a single zero eigenvalue so that the polarization vectors are uniquely determined. As long as the eigenvalues of a given matrix do not depend on the coordinate system used, let us represent the matrix  $M$  of the coefficients in Eq. (8) in spherical coordinates<sup>4</sup>:

$$M = -k_0 \begin{bmatrix} \epsilon_{rr} & \epsilon_{r\theta} & \epsilon_{r\varphi} \\ \epsilon_{\theta r} & \epsilon_{\theta\theta} - \hat{k}^2 & \epsilon_{\theta\varphi} \\ \epsilon_{\varphi r} & \epsilon_{\varphi\theta} & \epsilon_{\varphi\varphi} - \hat{k}^2 \end{bmatrix}, \quad (\text{A1})$$

where  $\hat{k} = k/k_0$ .

Let us assume that the zero eigenvalue of this matrix is not single. It cannot be triple, because in that case the matrix will be null. If there is a double zero eigenvalue of  $M$ , this means that its rows are not linearly independent and thus two of them can be expressed in terms of a single row, say, the first one:

$$\epsilon_{\theta r} = a \epsilon_{rr}, \quad \epsilon_{\theta\theta} - \hat{k}^2 = a \epsilon_{r\theta} \Rightarrow \hat{k}^2 = \epsilon_{\theta\theta} - \frac{\epsilon_{\theta r} \epsilon_{r\theta}}{\epsilon_{rr}}, \quad (\text{A2})$$

$$\epsilon_{\varphi r} = b \epsilon_{rr}, \quad \epsilon_{\varphi\varphi} - \hat{k}^2 = b \epsilon_{r\varphi} \Rightarrow \hat{k}^2 = \epsilon_{\varphi\varphi} - \frac{\epsilon_{\varphi r} \epsilon_{r\varphi}}{\epsilon_{rr}}. \quad (\text{A3})$$

As long as Eqs. (A2) and (A3) have to be simultaneously satisfied, this imposes a link between the elements of the permittivity tensor:

$$\epsilon_{\varphi\varphi} - \frac{\epsilon_{\varphi r} \epsilon_{r\varphi}}{\epsilon_{rr}} = \epsilon_{\theta\theta} - \frac{\epsilon_{\theta r} \epsilon_{r\theta}}{\epsilon_{rr}}. \quad (\text{A4})$$

However, if this condition is satisfied, it follows from Eq. (16) of Ref. 4 that the two wavenumbers  $k_1$  and  $k_2$  are identical. The conclusion is that if  $k_1 \neq k_2$ , there is a single zero eigenvalue of  $M$ , to which corresponds a unique eigenvector, which will determine the polarization vector. When  $k_1 = k_2$ , the zero eigenvalue is twice degenerated, there are two eigenvectors corresponding to this double eigenvalue, and they represent the two mutually orthogonal polarization vectors.

## APPENDIX B: ANALYTICAL DETERMINATION OF THE WAVE POLARIZATION VECTORS

Once the wavenumbers  $k_j$  ( $j=1,2$ ) are found, Eq. (8) will interrelate the components of  $\mathbf{A}_j$ . Let us, at first, take as an independent component  $A_{j,\rho} = \mathbf{A}_j \cdot \hat{\rho}$ . The case when this component is null will be analyzed separately.

Defining normalized wavenumbers  $\hat{k}_z = k_z/k_0$ , Eq. (8) is written as.

$$\begin{aligned} (\hat{k}_z^2 - \epsilon_{\rho\rho})A_{j,\rho} - \epsilon_{\rho\varphi}A_{j,\varphi} - (\hat{k}_z^2 t_j + \epsilon_{\rho z})A_{j,z} &= 0, \\ -\epsilon_{\varphi\rho}A_{j,\rho} + [\hat{k}_z^2(1 + t_j^2) - \epsilon_{\varphi\varphi}]A_{j,\varphi} - \epsilon_{\varphi z}A_{j,z} &= 0, \\ -(\hat{k}_z^2 t_j + \epsilon_{z\rho})A_{j,\rho} - \epsilon_{z\varphi}A_{j,\varphi} + (\hat{k}_z^2 t_j^2 - \epsilon_{zz})A_{j,z} &= 0. \end{aligned} \quad (\text{B1})$$

The fact that the determinant of this set is null means that there are at maximum two independent equations among the three. Let us assume that these are the first two equations, so that they give the required relations:

$$A_{j,\varphi} = \frac{\det \begin{bmatrix} k_z^2 - \epsilon_{\rho\rho} & \hat{k}_z^2 t_j + \epsilon_{\rho z} \\ \epsilon_{\rho\varphi} & -\epsilon_{\varphi z} \end{bmatrix}}{\det \begin{bmatrix} \epsilon_{\rho\varphi} & \hat{k}_z^2 t_j + \epsilon_{\rho z} \\ \hat{k}_z^2(1 + t_j^2) - \epsilon_{\varphi\varphi} & -\epsilon_{\varphi z} \end{bmatrix}} A_{j,\rho}, \quad (\text{B2})$$

$$A_{j,z} = \frac{\det \begin{bmatrix} \epsilon_{\rho\varphi} & \hat{k}_z^2 - \epsilon_{\rho\rho} \\ \hat{k}_z^2(1 + t_j^2) - \epsilon_{\varphi\varphi} & \epsilon_{\varphi\rho} \end{bmatrix}}{\det \begin{bmatrix} \epsilon_{\rho\varphi} & \hat{k}_z^2 t_j + \epsilon_{\rho z} \\ \hat{k}_z^2(1 + t_j^2) - \epsilon_{\varphi\varphi} & -\epsilon_{\varphi z} \end{bmatrix}} A_{j,\rho}. \quad (\text{B3})$$

The case when  $A_{j,\rho} = \mathbf{A}_j \cdot \hat{\rho} = 0$  greatly simplifies Eqs. (B1). In addition, to have a nontrivial solution ( $A_{j,\varphi} \neq 0$  and/or  $A_{j,z} \neq 0$ ), it is necessary that the determinant in the denominator of Eqs. (B2) and (B3) is null, i.e., that two of

the three equations in the set of Eqs. (B1) are linearly dependent. Let us take the second and third one:

$$\begin{aligned} [\hat{k}_z^2(1+t_j^2) - \epsilon_{\varphi\varphi}]A_{j,\varphi} - \epsilon_{\varphi z}A_{j,z} &= 0, \\ \epsilon_{z\varphi}A_{j,\varphi} - (\hat{k}_z^2 t_j^2 - \epsilon_{zz})A_{j,z} &= 0. \end{aligned} \quad (\text{B4})$$

The condition to have a determinant equal to zero gives a quadratic equation for  $t_j^2$ . Once its solutions are found, they are used in one of the equations in the set of Eqs. (B4) to determine the link between  $A_{j,\varphi}$  and  $A_{j,z}$ . The particular case when  $\epsilon_{\varphi z} = 0$  and/or  $\epsilon_{z\varphi} = 0$  is simplified further on, as Eqs. (B4) take the form

$$\begin{aligned} (\hat{k}_j^2 - \epsilon_{\varphi\varphi})A_{j,\varphi} &= 0, \\ (\hat{k}_{j,\rho}^2 - \epsilon_{zz})A_{j,z} &= 0 \end{aligned} \quad (\text{B5})$$

with the following nontrivial solution:

$$\begin{aligned} \hat{k}_1^2 = \epsilon_{\varphi\varphi} \Rightarrow A_{1,\varphi} \neq 0, \quad A_{1,z} = 0 \Rightarrow \Gamma_1 = \hat{\varphi}, \\ \hat{k}_{2,\rho}^2 = \epsilon_{zz} \Rightarrow A_{2,z} \neq 0, \quad A_{2,\varphi} = 0 \Rightarrow \Gamma_2 = \hat{z}. \end{aligned} \quad (\text{B6})$$

## REFERENCES

1. C. F. Bohren and D. R. Huffman, *Absorption and Scattering of Light by Small Particles* (Wiley-Interscience, 1998).
2. J. C. Monzon and N. J. Damaskos, "Two-dimensional scattering by homogeneous anisotropic rod," IEEE Trans. Antennas Propag. **AP-34**, 1243–1249 (1986).
3. J. C. Monzon, "Three-dimensional scattering by an infinite homogeneous anisotropic circular cylinder: a spectral approach," IEEE Trans. Antennas Propag. **AP-35**, 670–682 (1987).
4. B. Stout, M. Nevière, and E. Popov, "Mie scattering by an anisotropic object. I. Homogeneous sphere," J. Opt. Soc. Am. A **23**, 1111–1123 (2006).
5. S. N. Papadakis, N. K. Uzunoglu, and C. N. Capsalis, "Scattering of a plane wave by a general anisotropic dielectric ellipsoid," J. Opt. Soc. Am. A **7**, 991–997 (1990).
6. M. Nevière and E. Popov, *Light Propagation in Periodic Media: Differential Theory and Design* (Marcel Dekker, 2003), p. 383.
7. W. Press, S. Teukoloky, W. Vetterling, and B. Flannery, *Numerical Recipes in FORTRAN* (Cambridge U. Press, 1992), p. 455.
8. P. Boyer, E. Popov, M. Nevière, and G. Renversez, "Diffraction theory: application of the fast Fourier factorization to cylindrical devices with arbitrary cross section lighted in conical mounting," J. Opt. Soc. Am. A (to be published).
9. M. Born and E. Wolf, *Principles of Optics* (Cambridge U. Press, 1999).